A New Understanding of Demineralization: The Dynamics of Brushite Dissolution

Ruikang Tang,[†] Christine A. Orme,[‡] and George H. Nancollas*,[†]

Department of Chemistry, Natural Sciences Complex, University at Buffalo, The State University of New York, Buffalo, New York 14260, and Department of Chemistry and Materials Sciences, Lawrence Livermore National Laboratory, Livermore, California 94550

Received: March 12, 2003; In Final Form: July 21, 2003

In situ atomic force microscopic studies of brushite dissolution suggest an exactly analogous mechanism to that of crystallization in which embryo formation takes place only after critical conditions are reached. Experimentally, the relationship between the spreading rate of dissolution steps and their sizes is first measured and the elimination of active dissolution sites is observed at different undersaturations. The results reinforce our previous "self-inhibition" model in which the dissolution rates decrease with time and the reactions are effectively suppressed. The data suggest a metastable zone for dissolution in undersaturated solutions, and this is confirmed by constant composition dissolution experiments near equilibrium. Clearly, it is important to understand the mechanism of dissolution when attempts are made to measure, experimentally, the solubilities of sparingly soluble minerals. Surface dissolution pits not only play important roles in dissolution kinetics, but also they can directly influence crystal morphology.

Introduction

Compared with the well-established theories for mineral crystallization, dissolution has received much less attention.[1,2] Most studies assume that it is spontaneous, and that the reactions continue until true equilibrium is reached, implying that the rates should be constant when the undersaturation is maintained.[3−5] However, recent studies have shown that some biominerals are resistant to dissolution.[6−9] Since solubility equilibrium is usually approached through dissolution, similar findings made in previous solubility studies of biominerals required the introduction of a new intermediate "metastable state"[7−9] concept. The constant-composition method (CC),[10] a highly reproducible technique for kinetic studies of crystallization and dissolution of sparingly soluble salts, has also shown a similar unusual dissolution behavior of calcium phosphates in that the rates decreased considerably with time and the reactions were effectively suppressed, even though the solutions remained undersaturated.[11,12]

A new mechanism for the dissolution of sparingly soluble electrolytes has been suggested and discussed in a previous paper.[11] The model involves a mechanism exactly analogous to that of crystallization with the participation of critical conditions involving dissolution steps. It is well-known that crystallization does not occur spontaneously until nuclei reach a critical size, r^*, or the driving force (supersaturation) is sufficiently large. Rather, a metastable equilibrium condition persists during an "induction period", τ, before crystals are formed. If the simplifying assumption is made that τ is essentially concerned with classical nucleation, we can use eq 1,

$$\ln \tau \propto \left[C_1 + C_2 \frac{{\gamma_{SL}}^3}{k^3 T^3 (\ln S)^2} \right] \tag{1}$$

in which, C_1 and C_2 are independent constants, k is Boltzman's constant, T the temperature, and S the supersaturation. It has long been recognized that there is a close relationship between solubility and the interfacial energy, γ_{SL}.[13] During dissolution some neighboring ions on the surface are replaced by water molecules to form units that escape into the bulk solution. Higher values of γ_{SL} indicate a greater difficulty in forming such an interface between the solid and aqueous phases. Therefore, sparingly soluble salts in aqueous solution always have much higher interfacial free energy values than soluble salts.[14] As a result, they have relatively wide metastable supersaturated zones and large induction times; for hydroxyapatite, at $S = 18$, τ is about 10 h.[14]

In the well-established theories of crystallization, the free energy change of crystallization, ΔG, is usually expressed by eq 2:[3,5]

$$\Delta G = \frac{4\pi r^3}{3\Omega_V} \Delta g + 4\pi r^2 \gamma_{SL} \tag{2}$$

where r is the size of nucleus (assumed spherical) and Ω_v the molecular volume. Δg, the change in Gibbs energy per molecule, is given by eq 3:

$$\Delta g = kT \ln S \tag{3}$$

During nucleation from a supersaturated solution, the first term on the right side of eq 2 is negative, reflecting the decrease of chemical potential, but the second term is positive due to the creation of solid−liquid interfaces. Thus, the dependence of the Gibbs energy on the size, r, passes through a maximum, and the critical size, r^*, can be obtained using eq 4:

$$r^* = 2\gamma_{SL}\Omega_V / \Delta g \tag{4}$$

It follows that the critical size is proportional to the surface energy. Unfortunately, until the new demineralization model was suggested,[11] interfacial free energy considerations have been virtually ignored in discussions of demineralization, even though they are emphasized for mineralization.[15]

* Author to whom correspondence should be addressed. E-mail: ghn@acsu.buffalo.edu.
[†] The State University of New York, Buffalo.
[‡] Lawrence Livermore National Laboratory.

10.1021/jp0346312 CCC: $25.00
Published on Web 08/27/2003

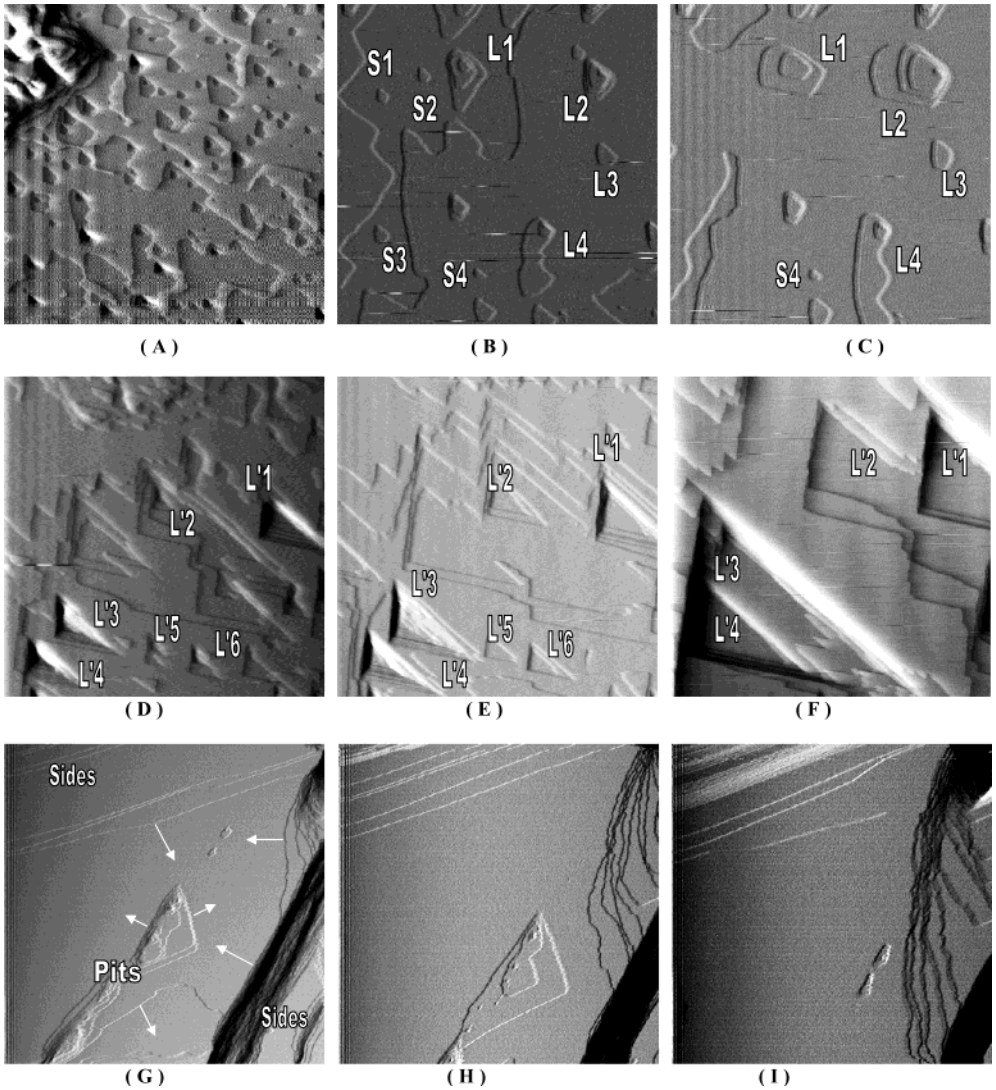

Figure 1. AFM movie frames of brushite dissolution on (010) surfaces. (A) shows the immediate formation of pits on the smooth surfaces of a crystallite introduced into undersaturated solutions of $\sigma = 0.060$; the scale of this image is $10 \times 10\ \mu$m. (B) and (C) show the subsequent developments of these pits, the intervals between (A), (B), and (C) are 6 min. (D)−(F) show the dissolving surface at a higher undersaturation of $\sigma = 0.172$, and intervals (D)−(E) and (E)−(F) are 3 and 6 min, respectively. (G)−(I) demonstrate that the sides of a neighboring large pit are dissolving back, removing layers from the top surface faster than new pits are nucleated. In this way the pits become more shallow and they are eventually removed from the dissolving surface. The time intervals are 3 min. The image scales of (B)−(I) are $5 \times 5\ \mu$m.

In the present work, the previously proposed critical dissolution step, the dependence of pit spreading rate on its size, the elimination of small pits by larger ones, and the size effect of small crystallites are observed and confirmed experimentally for brushite (dicalcium phosphate dihydrate, $CaHPO_4 \cdot 2H_2O$). These results consolidate the new demineralization model and explain the "abnormal" demineralization observations.

Experiment and Method

Brushite, a common biological mineral, may transform to the thermodynamically more stable hydroxyapatite by dissolution and reprecipitation.[16] In the present study, its dissolution mechanisms are examined under controlled solution conditions at physiological temperature, 37.0 ± 0.1 °C, and an ionic strength of 0.15 M. Details of the CC dissolution experiments and solution speciation calculations were described previously.[11,17] Values of association constants for formation of the ion pairs $CaH_2PO_4^+$, $CaHPO_4$, $CaPO_4^-$, and $CaOH^+$ were 28.1, 589, 1.40×10^6, and 25 M^{-1}, respectively.[11] The solubility activity product, K_{sp}, of brushite was 2.32×10^{-7} M^2.[16,18] The saturation ratio, S, and the relative undersaturation, σ, were defined as $(IP/K_{sp})^{1/2}$ and $1 - S$, respectively, where IP is the ionic activity product. High purity (>99.9%) brushite seed crystals were prepared as described elsewhere,[16,18] and the samples were characterized by chemical analysis, infrared, and X-ray diffraction.

A continuous-flow, single-pass wet atomic force microscope (AFM, MMAFM with a Nanoscope III controller, Digital Instruments) was used for the in situ dissolution investigation. Ion speciation of the flowing solutions were the same as those of the reaction solutions in CC experiments. The AFM was operated in contact mode using uncoated silicon cantilevers, and the continuous images were recorded.

Results and Discussions

When brushite crystallites are introduced into an understurated solution, AFM shows that numerous pits form immediately on the smooth crystal surfaces (Figure 1A), creating reactive dissolution sites. Similar pit creation has already been observed in previous studies,[19−21] and are analogous to nucleation on crystal surfaces with resultant hillock formation accompanying the first stages of crystal growth. The importance of pit

TABLE 1: Interfacial Energy Changes in a Number of Dissolution Cases

cases		$2\pi r\gamma$ (interfacial term)
dissolution from a hillock	away from source	decreases
	step containing source	unchanged if edge length is constant; or increases if edge length increases
pit creation from a flat surface		increases
dissolution from step sources with Burger's vectors perpendicular to surface		increases

formation and step flow during dissolution was also suggested by the results of recent studies.[11,22] AFM movie frames of (010) brushite crystal face dissolution (Figure 1) show the formation and growth of pits, the crystal surfaces becoming rougher and more irregular during dissolution. It is therefore not surprising to find that the interfacial energy term in eq 2 does not always decrease despite the reduction of crystallite sizes (Table 1). As a result, a critical condition for pit development exists analogously to eqs 2−4. This suggestion is supported by Figure 1, showing that only large pits (marked L1-4 and L′1-6 at low and high undersaturations, respectively) contribute to dissolution. Although small pits (marked S1-4) also exist on the surface, they are almost stationary in comparison with the large pits, and they make extremely small contributions to reaction (S4). Some of the small pits even disappear from the surface (S1-3) during dissolution and these can be regarded as having dimensions close to the critical size. It is also noted that the growth rates of the larger pits, L1, L2, and L′1-4, are greater than those of the smaller ones, e.g., L3, L′5, and L′6, implying a further dependence of dissolution rates on pit size. According to traditional theories of crystal growth,[3−5] the growth rates of nuclei and step lines, $R(r)$, are related to their sizes, r, through eq 5:

$$R(r) = R_\infty\left(1 - \frac{e^{\sigma r^*/r} - 1}{e^{\sigma} - 1}\right) \qquad (5)$$

in which R_∞ is the rate when r is infinitely large. Equation 5 shows that $R(r)$ increases with the sizes of nuclei and step lines. This relationship has been discussed in recent studies of calcite growth[23] and it may also be applied to other dissolution systems since the pits and nuclei all have similar features and roles. Figure 2 shows the relationship between the expanding velocities of pits and their sizes on dissolving (010) brushite faces as measured by AFM. At the lower relative undersaturation, 0.060, the experimental critical pit size is about 0.2 μm, since no pit growth occurs below this size. With an increase of pit size, $R(r)$ increases and tends to reach a relatively constant value, consistent with requirements of eq 5. Combining eqs 3 and 4, it can be seen that r^* decreases with increasing undersaturation. Due to the higher undersaturation and smaller critical size, the pits with zero developing rate cannot be observed directly on the rapidly dissolving brushite surface at $\sigma = 0.172$. However, an estimated value of r^*, 0.06−0.08 μm, can be obtained by extrapolating the experimental curve in Figure 2. This value is about one-fourth to one-third of that at $\sigma = 0.060$, in agreement with the predicted ratio, 0.328, from eqs 3 and 4.

Some smaller actively dissolving pits may be removed from the surface (see Figures 1G−1I) due to their proximity to much larger pits, which are developing more rapidly. Although new pits can be created on the dissolving surface, the energy required

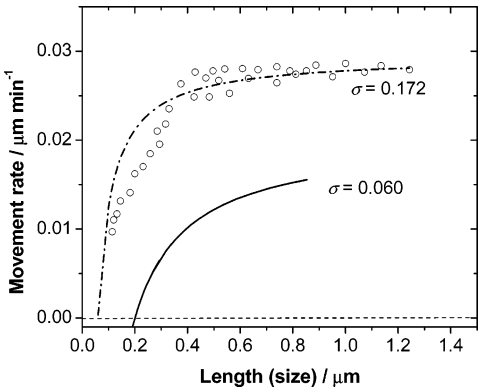

Figure 2. Plots of pit spreading velocities as a function of size on brushite dissolving surfaces, the data are measured from AFM frames at different experimental conditions. The solid and dashed curves are plotted according to eq 6.

will be appreciable, especially for sparingly soluble salts at low undersaturation. However, the development of existing large pits is spontaneous and will be favored during dissolution. Even if new pits do form in the rough dissolving surfaces, it is likely that they would be removed rapidly by existing dissolution steps prior to reaching a large size. Only a few newly created pits are found after dissolution is initiated; many more pits are removed from the dissolving surfaces. Comparing Figures 1B and 1C, the total number of dissolution sites is markedly reduced during dissolution; Figures 1D−1F show similar decreases of pit densities at higher undersaturation. Eventually, as dissolution continues, only a few large pits remain. However, sparingly soluble crystallites also usually have small sizes, in the order of micrometers. In our dissolution studies, the sizes of brushite seeds, 8−12 μm, were reduced markedly during dissolution. When the sizes of pits and crystallites were about the same, pit development was further limited by the crystallite sizes, and the resulting decreases of pit density and size result in the observed decrease of CC dissolution rate with time.[11,12] This interesting phenomenon demonstrates the self-inhibition by crystal size in the demineralization reactions.

Both the AFM experimental results and Birth-and-Spread (B + S) considerations imply that an effective dissolution model must include (i) the creation of pits, and (ii) pit spreading.[3] Near equilibrium, dissolution is always dominated by the latter step due to the low driving force and high critical energy for pit formation (eq 4).[12,24] As conditions deviate from the metastable region, the driving force increases, the critical energy decreases, and spontaneous pit creation is facilitated.[12,21] Previous studies have shown that nucleation on surfaces is the primary mechanism at high supersaturation,[24] whereas the spreading of existing step lines controls the reaction at low supersaturation.[3−5] Similar results have already been obtained for the dissolution of other calcium phosphates.[11,12,25] At high undersaturations, pit formation on the dissolving surfaces is facilitated to a greater degree and poly-pitting (etch pit formation) may control demineralization. Furthermore, with smaller values of r^* at the higher understaturations, for the same decrease in r (or the same crystallite mass loss, Δm), the change in the term $[1 - (e^{\sigma r^*/r} - 1)/(e^{\sigma} - 1)]$ is smaller and the critical dissolution conditions are not so apparent as at lower undersaturations (Figure 3A). However, this smaller rate reduction at higher undersaturation cannot be explained by traditional theories which only consider decreases in the number of dissolution sites[12] (Figure 1 shows that the density of active pits decreases more markedly at higher undersaturation). CC and solubility studies of biominerals have shown that dissolution reduction and termination are more

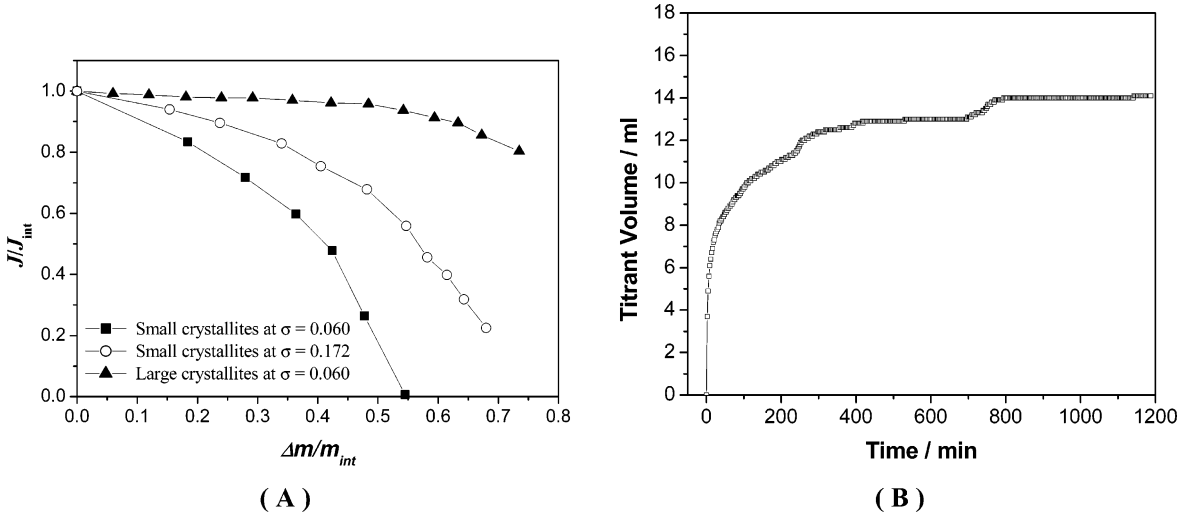

Figure 3. (A) Reduction of either crystallite size or undersaturation increases the extent of rate decrease, and the critical conditions become much more noticeable. Δm is the dissolved crystallite mass and m_{int}, the initial seed mass. The small brushite crystallites are 8−12 μm and the large ones, 40−60 μm. J, J_{int} are the dissolution rates at time t and $t = 0$, respectively. Expressed as moles of dissolved crystals per min per m^2, they are calculated from CC dissolution curves and normalized with respect to surface area. (B) Near solubility equilibrium ($\sigma = 0.016$), CC dissolution of brushite crystallites resumes after reaching the pseudo "equilibrium" states (the plateaus of the curve) over extended time periods, showing characteristic stepwise profiles. The titrant volume corresponding to complete dissolution would be about 55 mL.

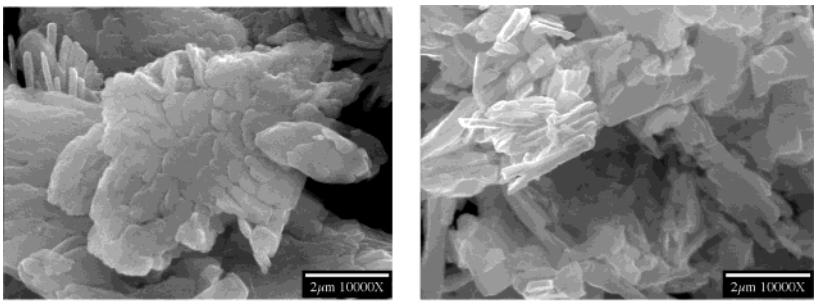

Figure 4. Scanning electron micrographs of brushite crystallites that have undergone dissolution at $\sigma = 0.060$ (A) and 0.172 (B).

apparent near equilibrium (low undersaturation).[6−9,11,12] However, these states are clearly thermodynamically unstable and the critical conditions for dissolution suppression cannot be sustained indefinitely. It can be seen in Figure 3B that over extended experimental times, dynamic dissolution resumes and a stepwise dissolution profile is obtained. Dissolution suppression and a pseudo solubility equilibrium appear at each plateau which can be considered as a metastable undersaturated zone near equilibrium. It should be emphasized that brushite has the highest solubility and lowest interfacial free energy of the calcium phosphates of interest. The thermodynamically more stable phases such as octacalcium phosphate and hydroxyaptite have much higher values of γ_{SL}.[14] For the former, similar stepwise dissolution behavior has been demonstrated at higher undersaturaiton, $\sigma \sim 0.2$.[11,12] In the case of hydroxyaptite, the metastable undersaturated zone can even reach $\sigma \sim 0.15$.[14]

Although it would be anticipated that all dissolution reactions would demonstrate similar behaviors, eqs 1−3 show that the critical condition is directly related to γ_{SL}, which, for the soluble salts, is much smaller, resulting in a much smaller r^* (usually in the order of a few nanometers), even at low undersaturation.[26,27] Moreover, by using relatively larger crystallites (on a mm scale) for the dissolution studies, their "abnormal" dissolution phenomena become much more difficult to investigate using available methodology. In the demineralization of brushite, even with the use of relatively large seed crystallites, the above critical phenomena are no longer noticeable (Figure 3A). Again, it can be seen that the critical dissolution behavior is only observed when crystallite and pit sizes are of the same order of magnitude. This may explain why mineral crystallites in biological systems are always submicron in size.

Another interesting phenomenon is the change of pit morphology at different undersaturations; this is isotropic (Figures 1A−1C) at lower undersaturation and anisotropic at higher driving force (Figure 1D−1F). As pits play fundamental dissolution roles, their morphologies would be reflected in the macro crystallites which have undergone dissolution. Figure 4 shows the scanning electron micrographs (SEM; Hitachi S-800) of brushite crystallites which have undergone dissolution at lower and higher undersaturations, respectively. At lower undersaturation, isotropic pits (Figures 1A−1C) result in large crystallites with irregular morphologies (Figure 4A); at high undersaturation the pits are triangular (Figure 1D−1F) with small, relatively regular crystallites (Figure 4B).

Conclusions

The experimental results support the new dissolution model of sparingly soluble electrolytes, which challenges the traditional understanding of demineralization. When the sizes of the crystallites are close to the values for critical dissolution steps, the dissolution can be suppressed and effectively inhibited by the crystallites themselves, resulting in the observed unusual dissolution profiles. Furthermore, even in undersaturated solutions, there are metastable zones for dissolution, which are more

apparent for sparingly soluble salts such as the biominerals. These have high surface tensions, large r^* values, and small crystallite sizes resulting in more readily attained critical conditions. The results suggest that these factors should be taken into account in determinations of the solubility of sparingly soluble electrolytes which may involve dissolution suppression and the existence of metastable undersaturated states. To attain "true" equilibrium solubility conditions, large crystallite size and long equilibrium times are recommended. Since the pits are the basic dissolution reaction units, it is also suggested that they not only play important roles in the kinetics of dissolution but they also directly influence crystal morphology.

Acknowledgment. We thank the National Institute of Dental and Craniofacial Research for Grant DE03223)in support of this research.

References and Notes

(1) Ohara, M.; Reid, R. C. *Modeling Crystal Growth Rates from Solution*; Prentice Hall: Englewood Cliffs, NJ, 1973.

(2) Stumm, W. *Chemistry of the Solid-Water Interface*; Wiley: New York, 1992.

(3) Hartman, P. *Crystal Growth: An Introduction*; North-Holland: Amsterdam-London-New York-Tokyo, 1975.

(4) Chernov, A. A. *Prog. Cryst. Growth Charact. Mater.* **1993**, *26*, 121.

(5) Hurle, D. T. J. *Handbook of Crystal Growth*; North-Holland: Amsterdam-London-New York-Tokyo, 1993.

(6) Barralet, J.; Akao, M.; Aoki, H. *J. Biomed. Mater. Res.* **2000**, *49*, 176.

(7) Driessens, F. C. M.; Verbeeck, R. M. H. *Z. Naturforsch* **1980**, *35*, 262.

(8) Baig, A. A.; Fox, J. L.; Wang, Z.; Higuchi, W. I.; Miller, S. C.; Barry, A. M.; Otsuka, R. *Calcified Tissue Int.* **1999**, *64*, 329.

(9) Zhuang, H.; Baig, A. A.; Fox, J. L.; Wang, Z. R.; Colby, S. J.; Chhettry, A.; Higuchi, W. I. *J. Colloid Interface Sci.* **2000**, *222*, 90.

(10) Tomson, M. B.; Nancollas, G. H. *Science* **1978**, *200*, 159.

(11) Tang, R.; Nancollas, G. H.; Orme, C. A. *J. Am. Chem. Soc.* **2001**, *123*, 5437.

(12) Zhang, J.; Nancollas, G. H. *Crystal Growth* **1992**, *123*, 59.

(13) Girifalco, L. A.; Good, R. J. *J. Phys. Chem.* **1957**, *61*, 904.

(14) Wu, W.; Nancollas, G. H. *Adv. Colloid Interface Sci.* **2000**, *79*, 229.

(15) Nielsen, A. E. *Kinetics of Precipitation*; The Macmillan Co.: New York, 1964.

(16) LeGeros, R. Z. *Calcium Phosphates in Oral Biology and Medicine*; S. Karger: Basel, 1991.

(17) Davies, C. W. *Ion Association*; Butterworth: London, 1962.

(18) Brown, W. E.; Lehr, J. R.; Smith, J. P.; Frazier, A. W. *J. Am. Chem. Soc.* **1957**, *79*, 5318.

(19) Malkin, A. J.; Kuznetsov, Yu. G.; Glantz, W.; Mcpherson, A. *J. Phys. Chem.* **1996**, *100*, 11736.

(20) Macherson, J. V.; Unwin, P. R.; Hillier, A. C.; Bard, A. J. *J. Am. Chem. Soc.* **1996**, *118*, 6445.

(21) Risthaus, P.; Bosbach, D.; Becker, U.; Putnis, A. *Colloid Surf. A* **2001**, *191*, 201.

(22) Jones, C. E.; Unwin, P. R.; Macpherson, J. V. *Chemphyschem* **2003**, *4*, 139.

(23) Teng, H. H.; Dove, P. M.; Orme, C. A.; De Yoreo, J. J. *Science* **1998**, *282*, 724.

(24) De Yoreo, J. J.; Land, T. A.; Rashkovich, L. N.; Onischenko, T. A.; Lee, J. D.; Monovskii, O. V.; Zaitseva, N. P. *J. Crystal Growth* **1997**, *182*, 442.

(25) Tang, R.; Wu, W.; Hass, M.; Nancollas, G. H. *Langmuir* **2001**, *17*, 3480.

(26) De Yoreo, J. J.; Land, T. A.; Dair, B. J. *Phys. Rev. Lett.* **1994**, *73*, 838.

(27) Land, T. A.; De Yoreo, J. J. *J. Crystal Growth* **2000**, *208*, 623.